

# Effect of uniform distributions of bonded and debonded fibers on the growth of the fiber/matrix interface crack in UD laminates with different fiber contents under transverse loading

Luca Di Stasio<sup>a,b</sup>, Janis Varna<sup>b</sup>, Zoubir Ayadi<sup>a</sup>

<sup>a</sup>Université de Lorraine, EEIGM, IJL, 6 Rue Bastien Lepage, F-54010 Nancy, France

<sup>b</sup>Luleå University of Technology, University Campus, SE-97187 Luleå, Sweden

---

## Abstract

*Priority: 1*

*Target journal(s):* Composites Part B: Engineering, Composites Part A: Applied Science and Manufacturing, Composite Structures, Journal of Composite Materials, Composite Communications

---

## 1. Introduction

1. We start with a few lines devoted to the spread tow technology and thin plies: what they are, what can be done, what are the possible applications.
- 5 2. By quoting the relevant references, we report on the observation that one of the main beneficial mechanisms in thin ply is the retardation of transverse crack propagation. We then enlarge by reporting the microscopical observations by Saito, in which debonds where also observed. We observe that available microscopic observations are just a few and mainly in 2D.
- 10 3. Propagation of transverse cracks has been widely investigated both analytically and numerically
4. Initiation at the level of fiber/matrix interface is instead a less researched subject.

5. cohesive elements are a possible choice, but have some drawbacks, which  
15 makes a LEFM approach valuable
6. With regard to LEFM studies of laminates under transverse loading, models can be found in the literature about: the single fiber in infinite matrix under different mode of loading, the effect of adjacent fibers on a fiber in infinite matrix under different mode of loading, the single fiber in an  
20 equivalent composite in transverse tension, the effect of adjacent fibers on a fiber in an equivalent composite in transverse tension.
7. For initiation of transverse cracking at the fiber/matrix interface in UD laminates under transverse tension, there is thus a gap regarding: the effect of fiber volume fraction; the interaction of debonded and bonded  
25 fibers in micro-structured assemblies, i.e. no homogenization. This article addresses these two points.
8. We conclude the introduction with a summary of the article's structure.

## 2. RVE models & FE discretization

### 2.1. Models of Representative Volume Element (RVE)

30 We start by describing the different idealized micro-structures considered and the corresponding repeating element or RVE used to model them. Fig. 1

### 2.2. Finite Element (FE) discretization

We describe the model implemented: schematic + description of parameters, formulation (LEFM, frictionless contact, VCCT, J-Integral), implementation of  
35 BCs, mesh. Fig. 2

### 2.3. Validation of the model

We mention once in this paper the validation of the model with respect to BEM results. Fig. 3

### 3. Results & Discussion

#### 40 3.1. Effect of Fiber Volume Fraction

The effect is similar for all the different BC cases, it's enough to show some of them to exemplify.  $G_I$  in Fig. 4,  $G_{II}$  in Fig. 5.

Graphics of ERR vs  $\Delta\theta$ , one curve for each  $V_f$ , one graphic for each selected BC. Selected BC: free, coupling, some examples with fibers (see captions).

#### 45 3.2. Interaction between debonds in UD laminates with a single layer of fibers

We start with a simpler (1 parameter: number of fibers in the horizontal directions) but more extreme model: one line of fibers. What's the effect on  $G_I$  and  $G_{II}$ ? It increases them: a compliant element in the middle of two stiffer ones. Reference to Kies strain magnification.  $G_I$  in Fig. 6,  $G_{II}$  in Fig. 7.

50 One graphic for each  $V_f$  (30%,50%,60%,65%), one curve for each case of fibers on the side (1, 2, 3, 5, 10, 50, 100).

#### 3.3. Influence of layers of fully bonded fibers on debond's growth in a centrally located line of debonded fibers

55 We then move to a ply with multiple lines of fibers and only debonded fibers in the central one (still only 1 parameter: number of fibers in vertical direction, but bit closer to real plies). No significant effect.  $G_I$  in Fig. 8,  $G_{II}$  in Fig. 9.

One graphic for each  $V_f$  (30%,50%,60%,65%), one curve for each case of fibers on top (1, 2, 3, 5, 10, 50, 100).

60

#### 3.4. Interaction between debonds in UD laminates with multiple layers of fibers

Finally models that are closer to real laminates and are more complex (2 parameters: number of fibers along the horizontal direction, number of layers in the vertical one).  $G_I$  in Fig. 10,  $G_{II}$  in Fig. 11.

65 One graphic for each  $V_f$  (30%,50%,60%,65%), one curve for some selected case of fibers on top and on the side. Hypothesis of selected cases ([n. on side,

n. on top]): [1,1], [2,1], [2,2], [5,1], [5,5], [10,1], [10,10], [50,1], [50,10], [100,1], [100,10]

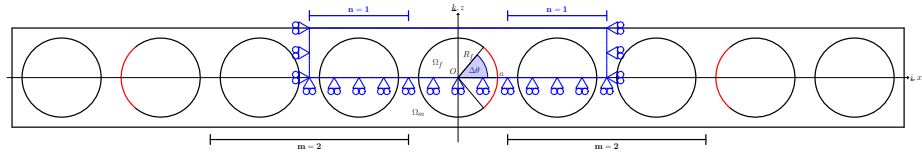
### 70 3.5. Comparison with the single fiber model with equivalent boundary conditions

We compare the previous results with the corresponding models of single fibers with equivalent BC. We draw conclusions on the possibility of using a single fiber with equivalent BCs. By remembering the actual ply configurations the repeating elements are modeling, and observing that in the vertical direction no significant effect related to the presence of debonded or bonded fiber can be found, we conclude that debonds appearing in fibers aligned in the vertical direction are energetically equivalent, and thus different configurations of debonded/bonded fibers along the vertical direction have the same probability. It is thus likely, from the energetic point of view, that debonds form at the same time along fibers aligned vertically.  $G_I$  in Fig. 12 and Fig. 14,  $G_{II}$  in Fig. 13 and Fig. 15.

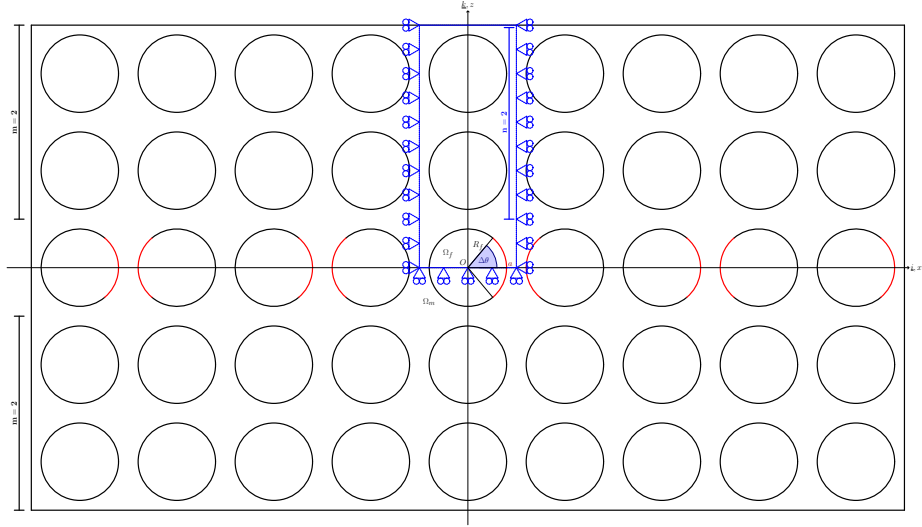
One graphic for each  $V_f$  (30%,50%,60%,65%), one curve for single fiber with BC + some selected case of fibers on top and on the side. Hypothesis of selected cases ([n. on side, n. on top]): [1,1], [2,1], [2,2], [5,1], [5,5], [10,1], [10,10]

85

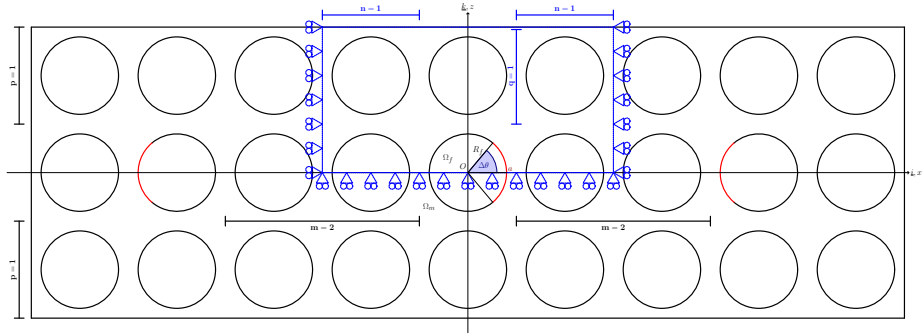
## 4. Conclusions & Outlook



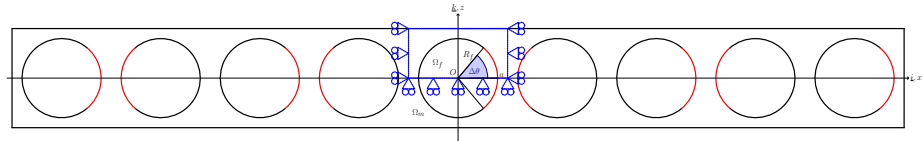
(a) Single layer of fibers with a debond appearing every  $m$  fibers.



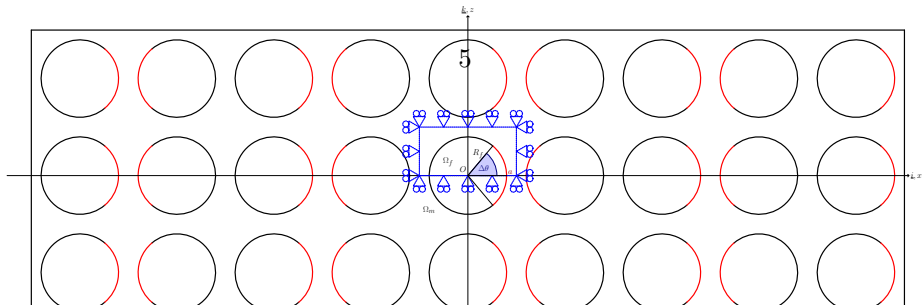
(b) Multiple layers of fibers with debonds appearing on each fiber belonging to the central layer.



(c) Multiple layers of fibers with a debond appearing every  $m$  fibers within the central layer.



(d) Single layer of fibers with debonds appearing on each fiber.



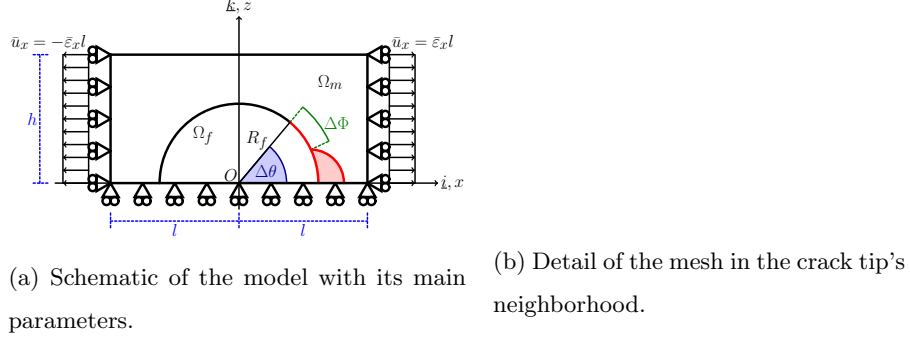


Figure 2: Details and main parameters of the Finite Element model.

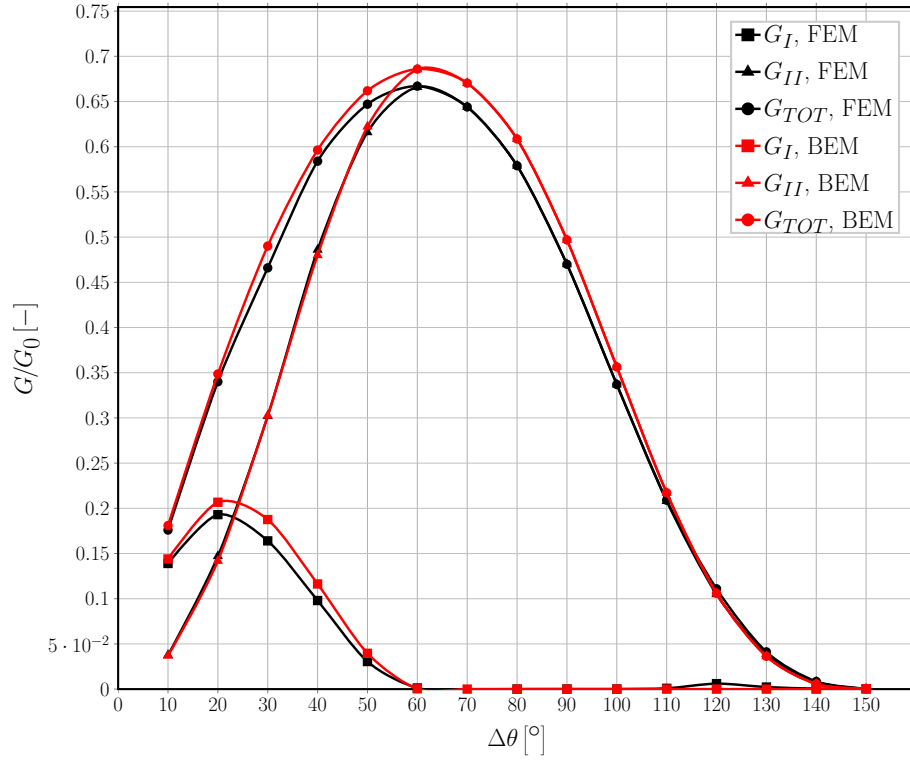


Figure 3: Validation of the single fiber model for the infinite matrix case with respect to the BEM solution in [1].

- |   |  |
|---|--|
| (a) Single fiber model with free boundary on top. | (b) Single fiber model with coupling of vertical displacements along the upper boundary. |
| (c) 1 fiber each side.                            | (d) 1 fiber above.   |
| (e) 5 fibers each side.                           | (f) 5 fibers above.  |
| (g) 10 fibers each side.                          | (h) 10 fibers above.   |
| (i) 1 fiber each side, 1 above.                   | (j) 3 fibers each side, 1 above.   |
| (k) 2 fibers each side, 2 above.                  | (l) 5 fibers each side, 2 above.   |

Figure 4: A view of the effect of fiber volume fraction on Mode I ERR across different models.

- |   |  |
|---|--|
| (a) Single fiber model with free boundary on top. | (b) Single fiber model with coupling of vertical displacements along the upper boundary. |
| (c) 1 fiber each side.                            | (d) 1 fiber above.   |
| (e) 5 fibers each side.                           | (f) 5 fibers above.  |
| (g) 10 fibers each side.                          | (h) 10 fibers above.   |
| (i) 1 fiber each side, 1 above.                   | (j) 3 fibers each side, 1 above.   |
| (k) 2 fibers each side, 2 above.                  | (l) 5 fibers each side, 2 above.   |

Figure 5: A view of the effect of fiber volume fraction on Mode II ERR across different models.

- |                    |                    |
|--------------------|--------------------|
| (a) $V_f = 30\%$ . | (b) $V_f = 50\%$ . |
| (c) $V_f = 60\%$ . | (d) $V_f = 65\%$ . |

Figure 6: Effect of the interaction between debonds appearing at regular intervals on Mode I ERR in a single-ply laminate with a single layer of fibers at different levels of fiber volume fraction  $V_f$ .

- (a)  $V_f = 30\%$ . (b)  $V_f = 50\%$ .  
(c)  $V_f = 60\%$ . (d)  $V_f = 65\%$ .

Figure 7: Effect of the interaction between debonds appearing at regular intervals on Mode II ERR in a single-ply laminate with a single layer of fibers at different levels of fiber volume fraction  $V_f$ .

- (a)  $V_f = 30\%$ . (b)  $V_f = 50\%$ .  
(c)  $V_f = 60\%$ . (d)  $V_f = 65\%$ .

Figure 8: Influence of layers of fully bonded fibers on debond's growth in Mode I ERR in a centrally located line of debonded fibers at different levels of fiber volume fraction  $V_f$ .

- (a)  $V_f = 30\%$ . (b)  $V_f = 50\%$ .  
(c)  $V_f = 60\%$ . (d)  $V_f = 65\%$ .

Figure 9: Influence of layers of fully bonded fibers on debond's growth in Mode II ERR in a centrally located line of debonded fibers at different levels of fiber volume fraction  $V_f$ .

- (a)  $V_f = 30\%$ . (b)  $V_f = 50\%$ .  
(c)  $V_f = 60\%$ . (d)  $V_f = 65\%$ .

Figure 10: Effect of the interaction between debonds appearing at regular intervals on Mode I ERR in a single-ply laminate with multiple layers of fibers at different levels of fiber volume fraction  $V_f$ .

- (a)  $V_f = 30\%$ . (b)  $V_f = 50\%$ .  
(c)  $V_f = 60\%$ . (d)  $V_f = 65\%$ .

Figure 11: Effect of the interaction between debonds appearing at regular intervals on Mode II ERR in a single-ply laminate with multiple layers of fibers at different levels of fiber volume fraction  $V_f$ .



- (a)  $V_f = 30\%$ . (b)  $V_f = 50\%$ .  
(c)  $V_f = 60\%$ . (d)  $V_f = 65\%$ .

Figure 12: Comparison of Mode I ERR between the single fiber model with free upper boundary and the multiple fibers model with fibers only on the side at different levels of fiber volume fraction  $V_f$ .

- (a)  $V_f = 30\%$ . (b)  $V_f = 50\%$ .  
(c)  $V_f = 60\%$ . (d)  $V_f = 65\%$ .

Figure 13: Comparison of Mode II ERR between the single fiber model with free upper boundary and the multiple fibers model with fibers only on the side at different levels of fiber volume fraction  $V_f$ .

- (a)  $V_f = 30\%$ . (b)  $V_f = 50\%$ .  
(c)  $V_f = 60\%$ . (d)  $V_f = 65\%$ .

Figure 14: Comparison of Mode I ERR between the single fiber model with coupling conditions along the upper boundary and the multiple fibers model with fibers above and both above and on the side at different levels of fiber volume fraction  $V_f$ .

- (a)  $V_f = 30\%$ . (b)  $V_f = 50\%$ .  
(c)  $V_f = 60\%$ . (d)  $V_f = 65\%$ .

Figure 15: Comparison of Mode II ERR between the single fiber model with coupling conditions along the upper boundary and the multiple fibers model with fibers above and both above and on the side at different levels of fiber volume fraction  $V_f$ .